



## Journal of Advanced Research in Fluid Mechanics and Thermal Sciences

Journal homepage:  
[https://semarakilmu.com.my/journals/index.php/fluid\\_mechanics\\_thermal\\_sciences/index](https://semarakilmu.com.my/journals/index.php/fluid_mechanics_thermal_sciences/index)  
ISSN: 2289-7879



# Investigating the Effects of Wu's Slip and Smoluchowski's Slip on Hybrid TiO<sub>2</sub>/Ag Nanofluid Performance

Lim Yeou Jiann<sup>1,\*</sup>, Sharena Mohamad Isa<sup>2</sup>, Noraihan Afiqah Rawi<sup>1</sup>, Ahmad Qushairi Mohamad<sup>1</sup>, Sharidan Shafie<sup>1</sup>

<sup>1</sup> Department Mathematical Sciences, Faculty Sciences, Universiti Teknologi Malaysia, Skudai, 81310 Johor Bahru, Johor, Malaysia

<sup>2</sup> Manufacturing Engineering Technology Section, Universiti Kuala Lumpur Malaysia Italy Design Institute (UniKL MIDI), Kuala Lumpur, 56100, Malaysia

### ARTICLE INFO

#### Article history:

Received 20 April 2023

Received in revised form 22 June 2023

Accepted 30 June 2023

Available online 15 July 2023

#### Keywords:

Wu's slip; temperature jump; hybrid nanofluid

### ABSTRACT

The high thermal conductivity of Titanium dioxide (TiO<sub>2</sub>) makes it ideal for heat transfer, particularly in a solar collector. However, nanofluids containing dissolved TiO<sub>2</sub> nanoparticles tend to agglomerate. Thus, nanoparticle silver (Ag) is used to stabilize the nanofluid. This study looks at a hybrid nanoparticle of TiO<sub>2</sub> and Ag, which are put into water to make a hybrid nanofluid, over a stretching plate. The effects of Wu's velocity slip and Smoluchowski's temperature slip are taken into consideration. Xue's thermal conductivity model for the hybrid nanofluid is employed. The governing equations are transformed by applying the similarity transformation technique and solved semi-analytically using the Homotopy Analysis Method. The effect of the multiple slips on the fluid profiles is graphically displayed and discussed. Results illustrate that the temperature profile is diminished by 42% due to Smoluchowski's temperature slip parameter, while the velocity profile is reduced by more than 40% due to the first and second-order Wu's slip parameters. These findings are important for optimizing the performance of the hybrid nanofluids. For example, in the solar collector, where a better understanding of heat transfer fluid characteristics can improve the stability of the hybrid nanofluid and the efficiency of eco-friendly energy storage.

## 1. Introduction

Solar thermal energy is one of the green alternatives for solving the vanishing of fossil fuels and the global warming problem. It is an effective alternative way in supplying the massive consumption of energy in maintaining the human quality of life criteria. Indeed, the performance of solar collectors has to be improved. The collection of solar energy has suffered various losses due to heat transmission. This deficiency can be overcome if the thermal properties of the heat transfer fluid (HTF) in the solar collector, which conventionally are the water, ethylene glycol (EG), and thermal oil, can be improved. Recently, the fluid containing nanoparticles, called nanofluid, has been the concentration of researchers as the inclusion of these nanoparticles has substantially improved the

\* Corresponding author.

E-mail address: [jiann@utm.my](mailto:jiann@utm.my)

<https://doi.org/10.37934/arfmts.107.2.236252>

thermophysical properties of the heat transfer liquid. The concept of nanofluid has gained recognition after the first proposed by Choi and Eastman [1]. They observed that the thermal conductivity of the HTF with copper nanoparticles is enhanced. Choi *et al.*, [2] detected that the thermal conductivity of the HTF was approximately improved twice by the nanoparticles. The investigation of the nano-HTF has remarkably increased since then. A recent study has demonstrated that the use of hybrid nanoparticles in fluid results in significantly improved heat transfer properties compared to pure nanofluids [3-6]. Maskeen *et al.*, [4] observed that the thermal conducted activity rate has been improved greater as a minor amount of various stabilized nanoparticles are mixed. Besides that, the increment of viscosity in fluid with nanoparticles has been reduced by the hybridization of the nanoparticles [7]. Several studies have extensively reviewed the potential use of hybrid nanofluids in solar energy storage and solar systems [8-12].

Xuan *et al.*, [13] experimentally explore the feature of the plasmonic hybrid nanoparticles Titanium dioxide/ Silver, (TiO<sub>2</sub>/Ag) and plasmonic nanofluids (Ag) or plasmonic nanofluids (TiO<sub>2</sub>) in solar energy absorption. They found that the nano-TiO<sub>2</sub> fluid has a lower temperature as compared to the hybrid nanofluid. Despite both nanofluid Ag and composite nanoparticles TiO<sub>2</sub>/Ag having the same temperature, the hybrid nanofluid offers a cost advantage. TiO<sub>2</sub> is chemically and thermally stable, readily available for purchase, and economically priced [14]. TiO<sub>2</sub> has good thermal conductivity and has frequently been used in thermal absorption. However, as compared with the metallic nanoparticle silver (Ag), TiO<sub>2</sub> has a lower thermal conductivity [15]. Moreover, TiO<sub>2</sub> is easy to agglomerate [14]. To overcome these shortages, Ag and TiO<sub>2</sub> are normally combined to provide a stabilized HTF [15,16]. Jamshed *et al.*, [17] used the hyperbolic tangent fluid model to investigate the properties of the heat-transmitting hybrid nanofluid. The thermal performance of a hybrid nanofluid composed of copper (Cu) and TiO<sub>2</sub> nanoparticles suspended in ethylene glycol (EG) was evaluated. The findings indicate that the hybrid nanofluid exhibits superior thermal performance. Kho *et al.*, [18] investigated the impact of viscous dissipation on hybrid nanofluid Cu/TiO<sub>2</sub> for two cases: along stretching and shrinking surface. Then the effect of a rotating sheet with shrinking and stretching on a three-dimensional hybrid nanofluid was discussed by Teh *et al.*, [19]. Reddy *et al.*, [20] acknowledged the convection flow of the hybrid TiO<sub>2</sub>/Ag hybrid nanofluids with water (H<sub>2</sub>O) as the based fluid inside an annulus cylinder. The effect of the magnetic field and heat generation were analyzed. Kho *et al.*, [21] studied the hybrid TiO<sub>2</sub>/Ag nanofluid over a stretchable wedge. The author detected that the thermal conductivity of the hybrid fluid is enhanced when the percentage of the TiO<sub>2</sub> in the hybrid fluid increase. A characteristic of the Ag nanofluid, TiO<sub>2</sub> nanofluid, and TiO<sub>2</sub>/Ag hybrid nanofluid was compared by Ahmad [22]. The volume fraction of the hybrid nanoparticle was observed to significantly affect thermal transmission.

The assumption of a smooth surface by most of the researchers in the literature appears impractical, especially when the nano-scaled particles are incorporated into the fluid. To fulfill the realistic, the slip effect at the surface of the solar collector must be considered. It has a significant impact on thermal and momentum distribution in the fluid. Wu [23] has yielded an improved slip model that demonstrates practical utility compared to existing models, including the Maxwell model, the 2nd order slip model, and the 1.5 order slip model. Fang and Aziz [24] had applied Wu's slip boundary condition to study the viscous fluid flow over a stretching sheet. The introduced slip effect was detected to decrease the wall shear stress and then change the movement of the liquid. Fang *et al.*, [25] extended the investigation to consider a shrinking sheet. Dual solutions of the velocity profiles were determined. Similar to the previous discussion, the finding showed that the fluid velocity and the skin friction at the surface are strongly dependent on the slip velocity. The effect of Wu's slip condition on a tangent hyperbolic nanofluid flow was discussed by Khan *et al.*, [26]. The results indicate that the velocity distribution is reduced by the slip and the rheology behavior of the

fluid. However, the temperature profile gives an opposite tendency. Shaw *et al.*, [27] investigated the impact of Wu's slip and irregular heat source on a nanofluid flow through a thin needle. Farooq *et al.*, [28] recently elucidated the characteristic of a bioconvection Williamson nanofluid under the impact of Wu's slip and Cattaneo-Christov heat flux over a cylinder. Much more discussion on Wu's slip boundary condition is shown in previous studies [29-35].

Le *et al.*, [36] and Assam *et al.*, [37] presented the concept of temperature jump to improve the accuracy of computational fluid dynamics in simulating the nonequilibrium hypersonic gas flow. Accordingly, the heat flux acting on the surface has a normal direction. Sajid *et al.*, [38] studied the influence of a temperature jump on the flow of Carreau fluid over a stretching plate. Then, Sajid *et al.*, [39] extended the work done by considering the effect of the stretchable surface on the Sutterby nanofluid fluid flow. The nanofluid's heat transfer rate was found to decrease the Smoluchowski's parameter increased. A similar trend was observed by Atif *et al.*, [40]. Atif *et al.*, [40] had studied the effect of the slip velocity and Smoluchowski temperature jump on a tangent hyperbolic nanofluid. The thermal transmission of a Sutterby hybrid nanofluid in solar energy was discussed by Hussain *et al.*, [41]. The authors detected that the temperature of the hybridization nanofluid is improved with a negative variation in Smoluchowski's parameter. Jamshed *et al.*, [42] applied a numerical approach to restudy the fluid problem of Hussain *et al.*, [41]. Different type of hybrid nanofluid was considered by Jamshed *et al.*, [42]. They found that the volume fraction of the hybrid nanoparticle has a positive function with the temperature field but an inverse tendency with the temperature slip effect.

The literature survey indicates that no efforts were made to study the tangent Hyperbolic hybrid nanofluid flows and heat transfer with the influence of Wu's slip and Smoluchowski temperature jump slip. Therefore, following previous studies, the present study aims to theoretically investigate the impact of those slip effects on a hybrid nano-HTF (TiO<sub>2</sub>/Ag) in a solar collector [17,20,40]. The developed partial governing equations of the proposed fluid problem are initially transformed into ordinary governing equations by the similarity transformation technique. The Homotopy analysis technique is then practised to determine the results. The most significant parameter that affects heat transmission and fluid flow is evaluated by conducting a parametric study for the embedded parameters. The present study's finding is essential in optimizing the performance of the hybrid nano-HTF in the solar collector.

## 2. Mathematical Formulation

A two-dimensional incompressible steady boundary layer tangent hyperbolic fluid flow over a stretching plate is discussed in the present research. The fluid is dissolved with a water-based hybrid nanofluid containing silver (Ag) and Titanium dioxide (TiO<sub>2</sub>) nanoparticles. Smoluchowski's temperature jump and Wu's slip on the surface of the plate are considered. As illustrated in Figure 1, the horizontal axis ( $x$ -axis) is oriented parallel to the surface of the plate, while the vertical axis ( $y$ -axis) is oriented perpendicular to the surface. Magnetic strength  $B_0$  is imposed vertically on the plate.  $T_\infty$  is assumed for the fluid that is located far from the plate, and the fluid is static at the initial. The rheology relationship of the hyperbolic tangent fluid is written as [17,26]:

$$\tau^* = \left\{ [\mu_\infty + \mu_0] \tanh(\Gamma \tilde{\gamma})^\alpha + \mu_\infty \right\} \tilde{\gamma} \quad (1)$$

where  $\mu_0$  is the zero-shear-rate viscosity,  $\tau^*$  is the stress tensor,  $\mu_\infty$  is the infinite-shear-rate viscosity,  $\Gamma$  is the time material constant, and  $\alpha$  is the power law index and  $\tilde{\gamma}$  is expressed as:

$$\tilde{\gamma} = \sqrt{\frac{1}{2} \sum_i \sum_j \tilde{\gamma}_{ij} \tilde{\gamma}_{ij}} = \sqrt{\frac{1}{2} \Pi} \quad (2)$$

where  $\Pi$  is the second invariant strain tensor. We consider  $\mu_\infty = 0$  in the constitutive Eq. (1) since the shear rate viscosity is impossible to infinite. Furthermore, the shear thinning effect is assumed, thus we take  $\Gamma \tilde{\gamma} < 1$ . Then, by binomial expansion, Eq. (1) becomes:

$$\tau^* = \mu_0 (1 + \alpha [\Gamma \tilde{\gamma} - 1]) \tilde{\gamma} \quad (3)$$

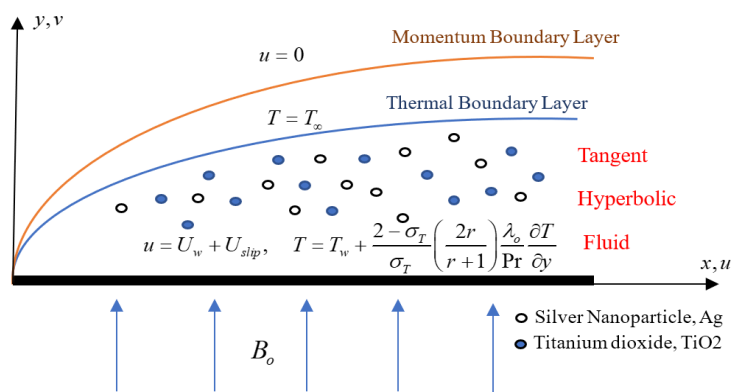


**Fig. 1.** The fluid flow of the hyperbolic tangent hybrid nanofluid through a stretchable sheet

The boundary layer approximation governing equations of the present considered tangent hyperbolic fluid are represented as:

$$\frac{\partial v}{\partial y} + \frac{\partial u}{\partial x} = 0, \quad (4)$$

$$v \frac{\partial u}{\partial y} + u \frac{\partial u}{\partial x} = \left( \frac{\mu}{\rho} \right)_{hmf} \left\{ (1-\alpha) \frac{\partial^2 u}{\partial y^2} + \Gamma \alpha \sqrt{2} \frac{\partial u}{\partial y} \frac{\partial^2 u}{\partial y^2} \right\} - \left( \frac{\sigma}{\rho} \right)_{hmf} B_0^2 u, \quad (5)$$

$$u \frac{\partial T}{\partial x} + v \frac{\partial T}{\partial y} = k_{hmf} \frac{\partial^2 T}{\partial y^2} + \left( \frac{\sigma}{\rho c_p} \right)_{hmf} B_0^2 u^2 + \left( \frac{\mu}{\rho c_p} \right)_{hmf} \left\{ (1-\alpha) \left( \frac{\partial u}{\partial y} \right)^2 + \frac{\alpha \Gamma}{\sqrt{2}} \left( \frac{\partial u}{\partial y} \right)^3 \right\}. \quad (6)$$

The heat capacitance, effective density, effective dynamics viscosity, and effective electrical conductivity of the hybrid nanofluid are indicated by  $(\rho c_p)_{hmf}$ ,  $\rho_{hmf}$ ,  $\mu_{hmf}$  and  $\sigma_{hmf}$  respectively. Following [23,27,40], the boundary conditions are:

$$\begin{aligned} u = U_w + U_{slip}, \quad v = 0, \quad T = T_w + T_{slip}, \quad \text{at} \quad y = 0, \\ u \rightarrow 0, \quad T \rightarrow T_\infty, \quad \text{as} \quad y \rightarrow \infty. \end{aligned} \quad (7)$$

where

$$U_w = \frac{ax}{l}, \quad T_{slip} = \frac{2\Lambda(2-\varpi_T)\beta}{\varpi_T(\Lambda+1)Pr} \frac{\partial T}{\partial y}$$

$$U_{slip} = \beta \left\{ \frac{2(3-\varpi_u I^2)}{3\varpi_u} - \frac{1-I^2}{K_n} \right\} \frac{\partial u}{\partial y} + \frac{\beta^2}{4} \left\{ \frac{2}{K_n^2}(I^2-1) - I^4 \right\} \frac{\partial^2 u}{\partial y^2} = A \frac{\partial u}{\partial y} + B \frac{\partial^2 u}{\partial y^2},$$

$a$  is a positive constant,  $\varpi_u$  and  $\varpi_T$  are the momentum and temperature accommodation coefficient, respectively,  $l$  is the characteristic length,  $\beta$  is the molecular mean free path, and  $\Lambda$  is the specific heat ratio.  $Pr$  is the Prandtl number and  $K_n$  is the Knudsen number and  $I$  is defined as  $\min(1/K_n, 1)$ .

The Eq. (4) - Eq. (7) are reduced into ordinary differential equations by using the following similarity variables;

$$\eta = y \sqrt{\frac{a}{l\nu_f}}, \quad \Phi = \sqrt{\frac{a\nu_f}{l}} xf(\eta), \quad u = \frac{\partial \Phi}{\partial y}, \quad v = -\frac{\partial \Phi}{\partial x}, \quad \theta = \frac{T-T_w}{T_w-T_\infty}, \quad (8)$$

where  $\nu_f$  is the fluid kinematic viscosity. Eq. (4) and Eq. (7) are converted into

$$ff'' - (f')^2 + \left(\frac{\nu_{hmf}}{\nu_f}\right) \left\{ (1-\alpha)f''' + \alpha We f'' f''' \right\} - \left(\frac{\sigma_{hmf} \rho_f}{\sigma_f \rho_{hmf}}\right) M^2 f' = 0 \quad (9)$$

$$\left(\frac{k_{hmf}}{k_f}\right) \theta'' + \left(\frac{\sigma}{\rho c_p}\right)_{hmf} \left(\frac{\rho c_p}{\sigma}\right)_f Pr Ec M^2 (f')^2 + \left(\frac{\nu}{c_p}\right)_{hmf} \left(\frac{c_p}{\nu}\right)_f \left\{ (1-\alpha) Pr Ec (f'')^2 + \frac{We}{2} \alpha Pr Ec (f'')^3 \right\} + Pr f \theta' = 0 \quad (10)$$

with boundary conditions

$$f(0) = 0, \quad f'(0) = 1 + \delta_1 f''(0) + \delta_2 f'''(0), \quad f'(\infty) = 0, \quad (11)$$

$$\theta(0) = 1 + \delta_3 \theta'(0), \quad \theta(\infty) = 0.$$

where the derivative with respect to  $\eta$  is represented by a prime symbol.  $(\rho c_p)_f$ ,  $\sigma_f$ ,  $\rho_f$  and  $\mu_f$  represent the heat capacitance, electrical conductivity, density, and dynamic viscosity of the fluid, respectively. The embedded parameters are defined as:

$$\begin{aligned}
 M^2 &= \frac{\sigma_f B_0^2}{\rho_f a} l \text{ (Magnetic Parameter)}, \quad We = \sqrt{\frac{2}{\nu_f}} \left(\frac{a}{l}\right)^{1/2} U_w \Gamma \text{ (Weissenberg Number)}, \\
 Pr &= \frac{\nu_f}{k_f} \text{ (Prandtl number)}, \quad Ec = \frac{U_w^2}{c_p (T_w - T_\infty)} \text{ (Eckert number)}, \\
 \delta_1 &= A \sqrt{\frac{a}{l\nu_f}}, \quad \delta_2 = B \frac{a}{l\nu_f} \text{ (1st and 2nd order velocity slip parameter)}, \\
 \delta_3 &= \frac{2 - \varpi_T}{\varpi_T} \left(\frac{2\Lambda}{\Lambda + 1}\right) \frac{\beta}{Pr} \sqrt{\frac{a}{l\nu_f}} \text{ (temperature slip parameter)}.
 \end{aligned} \tag{12}$$

For the hybrid nanofluid flow, the thermophysical formula is given as [18,20,43]:

$$\begin{aligned}
 \frac{\rho_{hnf}}{\rho_f} &= (1 - \phi_2) \left\{ (1 - \phi_1) + \phi_1 \frac{\rho_{s1}}{\rho_f} \right\} + \phi_2 \frac{\rho_{s2}}{\rho_f}, \quad \frac{\mu_{hnf}}{\mu_f} = \frac{1}{(1 - \phi_1)^{2.5} (1 - \phi_2)^{2.5}}, \\
 \frac{\sigma_{hnf}}{\sigma_{bf}} &= \frac{\sigma_{s2} + 2\sigma_{bf} - 2\phi_2(\sigma_{bf} - \sigma_{s2})}{\sigma_{s2} + 2\sigma_{bf} + \phi_2(\sigma_{bf} - \sigma_{s2})}, \quad \text{where } \frac{\sigma_{bf}}{\sigma_f} = \frac{\sigma_{s1} + 2\sigma_f - 2\phi_1(\sigma_f - \sigma_{s1})}{\sigma_{s1} + 2\sigma_f + \phi_1(\sigma_f - \sigma_{s1})}, \\
 \frac{(\rho c_p)_{hnf}}{(\rho c_p)_f} &= (1 - \phi_2) \left\{ (1 - \phi_1) + \phi_1 \frac{(\rho c_p)_{s1}}{(\rho c_p)_f} \right\} + \phi_2 \frac{(\rho c_p)_{s2}}{(\rho c_p)_f}.
 \end{aligned} \tag{13}$$

The thermophysical properties of the based fluid and the hybrid nanoparticles are given in Table 1. The Xue model [44, 45] of thermal conductivity is given as

$$\begin{aligned}
 \frac{k_{hnf}}{k_{bf}} &= \left[ 1 - \phi_2 + 2\phi_2 \left( \frac{k_{s2}}{k_{s2} - k_{bf}} \right) \ln \left( \frac{k_{s2} + k_{bf}}{2k_{bf}} \right) \right] \left[ \left[ 1 - \phi_2 + 2\phi_2 \left( \frac{k_{bf}}{k_{s2} - k_{bf}} \right) \ln \left( \frac{k_{s2} + k_{bf}}{2k_{bf}} \right) \right] \right]^{-1}, \\
 \frac{k_{bf}}{k_f} &= \left[ 1 - \phi_1 + 2\phi_1 \left( \frac{k_{s1}}{k_{s1} - k_f} \right) \ln \left( \frac{k_{s1} + k_f}{2k_f} \right) \right] \left[ \left[ 1 - \phi_1 + 2\phi_1 \left( \frac{k_f}{k_{s1} - k_f} \right) \ln \left( \frac{k_{s1} + k_f}{2k_f} \right) \right] \right]^{-1},
 \end{aligned} \tag{14}$$

where  $\phi_1$  is the volume fraction of the Ag nanoparticle and  $\phi_2$  is for the TiO<sub>2</sub> nanoparticle.  $Re_x = ax^2 (l\nu_f)^{-1}$  is the Reynold number. The physical quantity of interest local skin friction ( $\frac{1}{2} C_f Re_x^{1/2}$ ) and the local Nusselt number ( $Nu Re_x^{-1/2}$ ), are denoted by

$$C_f Re_x^{1/2} = \frac{\nu_{hnf}}{\nu_f} \left[ (1 - \alpha) f''(0) + \frac{\alpha}{2} We f''(0) \right]^2, \quad Nu Re_x^{-1/2} = -\frac{k_{hnf}}{k_f} \theta'(0). \tag{15}$$

**Table 1**

The thermophysical properties of the water, H<sub>2</sub>O base fluids, and silver Ag and Titanium dioxide, TiO<sub>2</sub>, nanoparticles [5,20,21]

Base fluid and Nanoparticles	H <sub>2</sub> O	Ag	TiO <sub>2</sub>
$\rho [kg \cdot m^{-3}]$	997.1 $[\rho_f]$	10500, $[\rho_{s1}]$	4250, $[\rho_{s2}]$
$\sigma [\Omega^{-1} \cdot m^{-1}]$	0.055, $[\sigma_f]$	$6.3 \times 10^7$ , $[\sigma_{s1}]$	$2.6 \times 10^6$ , $[\sigma_{s2}]$
$k [W \cdot m^{-1} \cdot K^{-1}]$	0.613, $[k_f]$	429, $[k_{s1}]$	8.953, $[k_{s2}]$
$(c_p) [J \cdot kg^{-1} \cdot K^{-1}]$	4179, $[(c_p)_f]$	235, $[(c_p)_{s1}]$	686.2, $[(c_p)_{s2}]$

### 3. Homotopy Analysis Solutions

The governing Eq. (9) – Eq. (11) are solved by using the Homotopy analysis method (HAM). The solutions are assumed to be functions  $f(\eta; p)$  and  $\theta(\eta; p)$  that depends on an embedded parameter  $p$ . The solutions can be expanded at  $\eta = 0$  by using Taylor's series expansion and produce

$$f(\eta; p) = f_0(\eta) + \sum_{m=1}^{\infty} f_m(\eta)p^m, \quad \theta(\eta; p) = \theta_0(\eta) + \sum_{m=1}^{\infty} \theta_m(\eta)p^m, \quad (16)$$

where

$$f_m(\eta) = \frac{1}{m!} \left. \frac{\partial^m f(\eta; p)}{\partial p^m} \right|_{p=0}, \quad \theta_m(\eta) = \frac{1}{m!} \left. \frac{\partial^m \theta(\eta; p)}{\partial p^m} \right|_{p=0}. \quad (17)$$

The solutions (16) are assumed converge to  $f(\eta)$  and  $\theta(\eta)$  respectively, at  $p = 1$  and possess analytic in  $p \in [0,1]$ . Therefore, we have;

$$\begin{aligned} \text{at } p=0, \quad & \theta(\eta; p) = \theta_0(\eta), \quad f(\eta; p) = f_0(\eta), \\ \text{at } p=1, \quad & \theta(\eta; p) = \theta(\eta), \quad f(\eta; p) = f(\eta). \end{aligned} \quad (18)$$

The solutions are:

$$f(\eta) = f_0(\eta) + \sum_{m=1}^{\infty} f_m(\eta), \quad \theta(\eta) = \theta_0(\eta) + \sum_{m=1}^{\infty} \theta_m(\eta). \quad (19)$$

The initial guesses are taken as:

$$f_0(\eta) = \frac{1 - e^{-\eta}}{1 + \delta_1 - \delta_2}, \quad \theta_0(\eta) = \frac{e^{-\eta}}{1 + \delta_3}, \quad (20)$$

The zeroth-order deformation of the governing equations are

$$(1-p)L_f \{f(\eta; p) - f_0(\eta)\} = p\hbar_f N_f \{f(\eta; p)\}, \quad (21)$$

$$(1-p)L_\theta \{ \theta(\eta; p) - \theta_0(\eta) \} = p \hbar_\theta N_\theta \{ f(\eta; p), \theta(\eta; p) \}. \quad (22)$$

$\hbar_\theta$  and  $\hbar_f$  are known as the convergence parameters for the heat equation and momentum equation, respectively. These parameters play a crucial role in defining the convergence rate of solutions to these equations.  $L_f$  and  $L_\theta$  are the linear differential operators and are presented as

$$L_f = \frac{\partial^3 f}{\partial \eta^3} + \frac{\partial^2 f}{\partial \eta^2}, \quad L_\theta = \frac{\partial^2 \theta}{\partial \eta^2} + \frac{\partial \theta}{\partial \eta}. \quad (23)$$

$N_f$  and  $N_\theta$  are nonlinear operators and are defined as

$$N_f \{ f(\eta; p) \} = \left( \frac{v_{hmf}}{v_f} \right) f'''(\eta; p) \{ (1-\alpha) + \alpha We f''(\eta; p) \} - [f'(\eta; p)]^2 + f(\eta; p) f''(\eta; p) - M^2 \left( \frac{\sigma_{hmf} \rho_f}{\sigma_f \rho_{hmf}} \right) f'(\eta; p), \quad (24)$$

$$N_\theta \{ f(\eta; p), \theta(\eta; p) \} = \left( \frac{v}{c_p} \right)_{hmf} \left( \frac{c_p}{v} \right)_f \left\{ (1-\alpha) Pr Ec f''(\eta; p)^2 + \frac{We}{2} \alpha Pr Ec f''(\eta; p)^3 \right\} + \left( \frac{k_{hmf}}{k_f} \right) \theta''(\eta; p) + \left( \frac{\sigma}{\rho c_p} \right)_{hmf} \left( \frac{\rho c_p}{\sigma} \right)_f Pr Ec M^2 f'(\eta; p)^2 + Pr f(\eta; p) \theta'(\eta; p), \quad (25)$$

$f_m$  and  $\theta_m$  are calculated by differentiating  $m$ -times with respect to  $p$  of the Eq. (21) and Eq. (22), and dividing them by  $m!$  respectively. Then, the  $m$ -th order deformation equations are obtained by taking  $p = 0$ , and we have

$$L_f \{ f_m(\eta) - \chi_m f_{m-1}(\eta) \} = \hbar_f \left\{ \left( \frac{v_{hmf}}{v_f} \right) \left\{ (1-\alpha) f_{m-1}''' + \alpha We \left[ \sum_{i=0}^{m-1} f_{m-1-i}'' f_i'' \right] \right\} + \left[ \sum_{i=0}^{m-1} f_{m-1-i} f_i'' \right] - \left[ \sum_{i=0}^{m-1} f_{m-1-i}' f_i' \right] - \left( \frac{\sigma_{hmf} \rho_f}{\sigma_f \rho_{hmf}} \right) M^2 f_{m-1}' \right\}. \quad (26)$$

$$L_\theta \{ \theta_m(\eta) - \chi_m \theta_{m-1}(\eta) \} = \hbar_\theta \left\{ \left( \frac{v}{c_p} \right)_{hmf} \left( \frac{c_p}{v} \right)_f \left\{ (1-\alpha) Pr Ec \sum_{i=0}^{m-1} f_{m-1-i}'' f_i'' + \sum_{i=0}^{m-1} f_{m-1-i}'' \frac{We}{2} \alpha Pr Ec \sum_{j=0}^i f_{i-j}'' f_j'' \right\} + \left( \frac{k_{hmf}}{k_f} \right) \theta_{m-1}'' + Pr \left( \sum_{i=0}^{m-1} f_{m-1-i} \theta_i' + \left( \frac{\sigma}{\rho c_p} \right)_{hmf} \left( \frac{\rho c_p}{\sigma} \right)_f Ec M^2 \sum_{i=0}^{m-1} f_{m-1-i}' f_i' \right) \right\}. \quad (27)$$

where  $\chi_m = 0$  ( $k \leq 1$ ),  $1$  ( $k > 1$ ). Eq. (26) and Eq. (27) are commonly known as high-order deformation equations. Solving Eq. (28) and Eq. (29) give the solutions of the  $f_m$  and  $\theta_m$ , respectively. The Mathematica package BVP4c 2.0 developed by S.J. Liao [46, 47] was employed to calculate the  $\theta_m$  and  $f_m$  for  $k \geq 1$ .



#### 4. Results

The current study has discussed the impact of Wu’s slip and Smoluchowski’s temperature slip on a magnetohydrodynamic hyperbolic tangent hybrid nanofluid flow on a stretchable plate. The water is used as the based fluid, and the commonly used nanoparticle silver, Ag, and Titanium dioxide, TiO<sub>2</sub> in the solar collector are dissolved in the fluid to form the tangent hyperbolic hybrid nanofluid. The parameters  $Pr = 7.38$ ,  $M = 0.1$ ,  $We = 0.2$ ,  $\alpha = 0.2$ ,  $\delta_1 = 0.5$ ,  $\delta_2 = -0.5$ ,  $\delta_3 = 0.1$ ,  $Ec = 0.2$ ,  $\phi_1 = 0.01$  and  $\phi_2 = 0.01$  are utilized as default for the analysis. Besides that, following previous studies, the parameters are taken in range  $\phi_1 = \phi_2 = \{0.01, 0.02, 0.03, 0.04\}$ ,  $\delta_1 = \delta_3 = \{0.1, 0.5, 1.0, 1.5, 2.0\}$ ,  $\delta_2 = \{-0.5, -1.0, -1.5, -2.0\}$ , to investigate fluid flow behavior and heat transfer [27,40,42,48,49].

Table 2 shows the convergences test of the approximation order used in the HAM. As depicted in the table, the solutions of the local skin friction and the local Nusselt number do not show large differences when the order of the approximation is increased from 10 to 50. The error between the solutions for both physical interests is more than  $1 \times 10^{-4}$  after order 30. Therefore, the solutions presented in this study were computed using a 30th-order approximation, which is much more efficient for time consumption. The precision of the proposed solutions has been validated by benchmarking them against results from the literature in specific situations. By taking  $We = \alpha = \delta_1 = \delta_2 = 0$ , the computed local  $C_f$  solutions for different magnetic strengths,  $M$  is found well agree with the results given in previous studies [49-52]. The comparison is illustrated in Table 3. Furthermore, Table 4 depicts that the results for the local Nusselt number are consensus with the finding in previous studies for  $Pr = 1,3,5,10$  [49,53,54]. This has validated and verified the computed solutions in the present investigation and further enhances the reliability of the analysis and discussion.

**Table 2**

Convergence test  $Pr = 7.38$ ,  $\alpha = We = Ec = 0.2$ ,  $M = 0.1$ ,  $\delta_1 = 0.5$ ,  $\delta_2 = -0.5$ ,  $\delta_3 = 0.1$ ,  $\phi_2 = 0.01$

$m$	$C_f$	$Nu$	Time Consume (s)
10	-0.483182	-0.694297	5.56138
20	-0.483109	-0.689064	18.7434
30	-0.483065	-0.688776	45.4952
40	-0.483057	-0.688978	86.971
50	-0.483055	-0.689197	151.992

**Table 3**

Validation for  $We = \alpha = \delta_1 = \delta_2 = 0$

$M$	Akbar <i>et al.</i> , [50]	Fathizadeh <i>et al.</i> , [52]	Ibrahim [51]	Ganesh <i>et al.</i> , [49]	Present
0	1	1	1	-	1
1	-1.41421	-1.41421	-1.41421	-1.41421	-1.41415
5	-2.44948	-2.44948	-2.44958	-2.44949	-2.44949
10	-3.31662	-3.31662	-3.31660	-3.31662	-3.31660

**Table 4**

Validation for  $M = We = Ec = \alpha = \delta_3 = 0$

$Pr$	Ali [53]	Chen [54]	Ganesh <i>et al.</i> , [49]	Present
1	-0.5801	-0.58199	-0.58223	-0.58347
3	-1.1599	-1.16523	-1.16522	-1.16573
5	-	-	-1.56803	-1.56810
10	-2.2960	-2.30796	-2.30798	-2.30951

The effect of the volume fraction of the nanoparticles on the fluid flow and heat transfer is recognized in Figure 2 and Figure 3. Comparing Figure 2(b) and Figure 3(b), the increment of the volume fraction of nanoparticles silver (Ag),  $\phi_1$  has generated a much alteration to the temperature distribution. This is because nanoparticle Ag has a higher thermal conductivity. Though the change in velocity profile is small, a contrary phenomenon is observed for both nanoparticles. Figure 2(a) illustrates that the velocity of the fluid is increased by the volume fraction  $\phi_1$  but  $\phi_2$  reduces the distribution, as seen in Figure 3(a). This variation happens because the inclusion of the nanoparticles in the fluid has physically changed the density of the fluid and increased the collision between the nanoparticles [55].

The influence of Wu's slip on the velocity profile of the fluid is given in Figure 4(a) and Figure 5(a). The first and second-order velocity parameters,  $\delta_1$  and  $\delta_2$ , have reduced the velocity profile. According to Fang and Aziz, [24] and Fang *et al.*, [25], the slip velocity in the first order gives physically meaningful results with a positive value and the slip velocity in the second order only happens when the number is in the negative root. The figures have shown that the impact of the  $\delta_2$  is more significant than the first-order velocity slip.  $\delta_1$  has reduced the velocity profile by about 43.33% when the number is changed from 0.5 to 2.0. On the other hand, 51.61% of the velocity profile is decreased when the number of  $\delta_2$  altered from -0.5 to -2.0. The effect of Wu's velocity slip on the temperature distribution reversely behaves, as demonstrated in Figure 4(b) and Figure 5(b). Either the increment of the first-order slip parameter or the decrement of the second-order slip velocity has increased the resistance to the velocity. Thus, the velocity profiles show a negative function with  $\delta_1$  and  $\delta_2$ , respectively, but a positive function with the temperature distribution. Li *et al.*, [35] had observed alike characteristics.

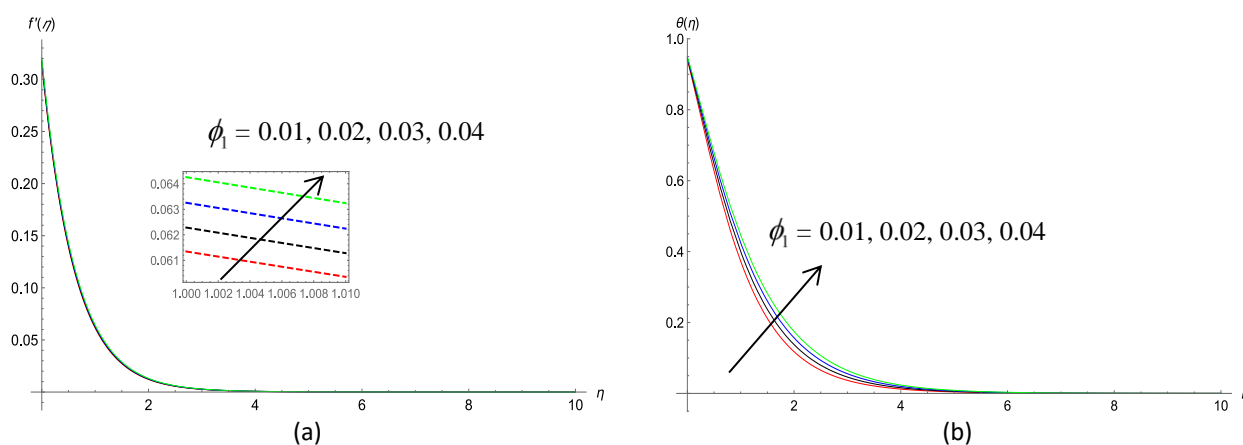


**Fig. 2.** Profile of different  $\phi_1$  values with  $M = 0.1$ ,  $We = 0.2$ ,  $\alpha = 0.2$ ,  $\delta_2 = -0.5$ ,  $\delta_1 = 0.5$ , and  $\phi_2 = 0.01$   
 (a) Velocity (b) Temperature

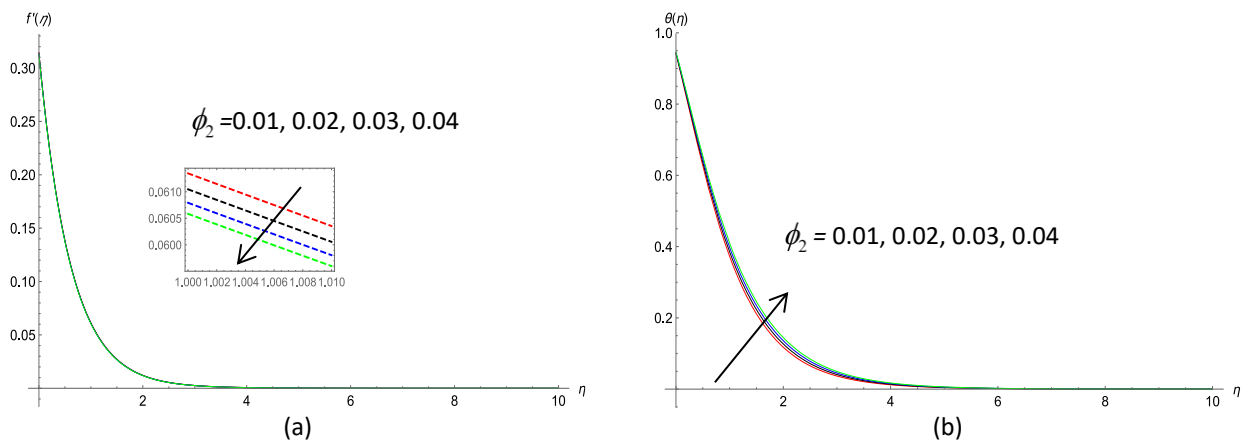


**Fig. 3.** Profile for different  $\phi_2$  values with  $M = 0.1$ ,  $We = 0.2$ ,  $\alpha = 0.2$ ,  $\delta_1 = 0.5$ ,  $\delta_2 = -0.5$ , and  $\phi_1 = 0.01$   
 (a) Velocity (b) Temperature

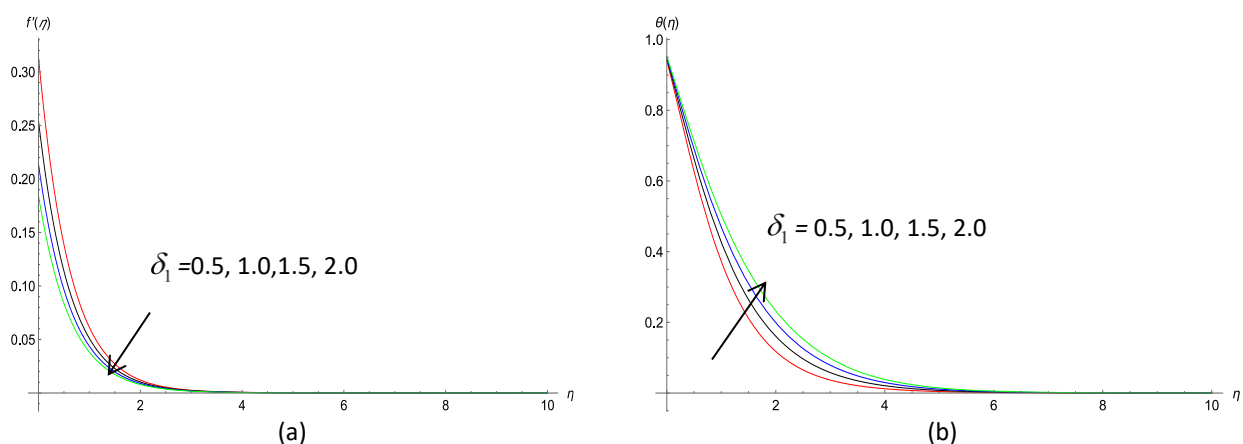


**Fig. 4.** Distribution for various  $\delta_1$  values with  $M = 0.1$ ,  $We = 0.2$ ,  $\alpha = 0.2$ ,  $\delta_2 = -0.5$ ,  $\phi_1 = 0.01$ , and  $\phi_2 = 0.01$  (a) Velocity and (b) Temperature

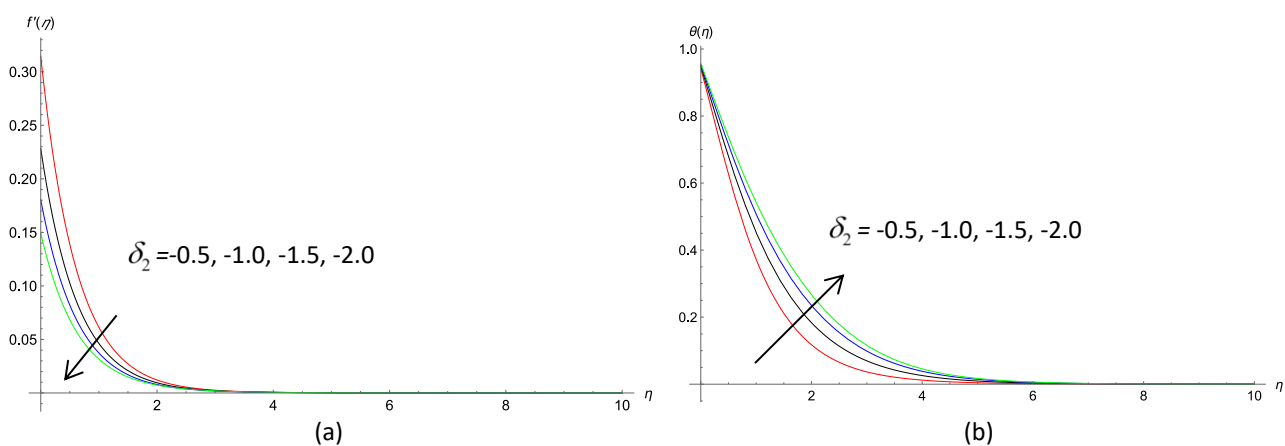


**Fig. 5.** Profile for different  $\delta_2$  values with  $M = 0.1$ ,  $We = 0.2$ ,  $\alpha = 0.2$ ,  $\delta_1 = 0.5$ ,  $\phi_1 = 0.01$ , and  $\phi_2 = 0.01$  (a) Velocity (b) Temperature

The effect of the temperature slip parameter is shown in Figure 6. The temperature profile is decreased by 42% when the number of the parameter  $\delta_3$  increase from 0.1 to 1.5. A larger value  $\delta_3$  reduces the conduction area of the plate surface with the ambient fluid. Thus, the heat transfer from the plate to the fluid is decreased due to the fluid temperature decline [41,42].

Table 5 demonstrates the characteristic of the local skin friction,  $C_f Re_x^{1/2}$  due to the alteration of the embedded parameters. The parameters  $M$ ,  $We$ ,  $\alpha$  and  $\delta_1$  give a positive function with the local skin friction. Besides that, the decrease of  $\delta_2$  from -0.5 to -2.0 has also enhanced the value of  $C_f Re_x^{1/2}$ . On the other hand, the value of the local skin friction is reduced by the volume fraction of the nanoparticles  $\phi_1$  and  $\phi_2$  respectively. The  $\phi_1$  and  $\phi_2$ , have enhanced the heat transfer rate as displayed in Table 6. The increase  $\phi_1$  and  $\phi_2$  from 0.01 to 0.04 has improved the heat transfer rate by 12.58% and 2.01%, respectively. The nanoparticle silver Ag has much increment because the material has a higher thermal conductivity. The second order Wu's slip parameter  $\delta_2$  has diminished the local Nusselt number,  $Nu Re_x^{-1/2}$ . Similar to the parameter  $M$ ,  $We$ ,  $\alpha$ ,  $Ec$ ,  $\delta_1$  and  $\delta_3$  decrease the number of the  $Nu Re_x^{-1/2}$ .

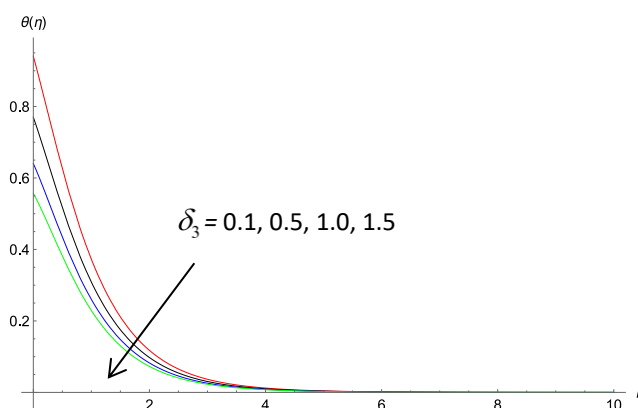


**Fig. 6.** Temperature profile for different  $\delta_3$  values with  $M = 0.1$ ,  $We = 0.2$ ,  $\alpha = 0.2$ ,  $\delta_1 = 0.5$ ,  $Ec = 0.2$ ,  $\phi_1 = 0.01$ , and  $\phi_2 = 0.01$

**Table 5**

Local Skin Friction for various embedding parameter values

$M$	$We$	$\alpha$	$\delta_1$	$\delta_2$	$\phi_1$	$\phi_2$	$Cf/Re$
0.1	0.2	0.2	0.5	-0.5	0.01	0.01	-0.483065
			1.0				-0.385783
			1.5				-0.320909
			2.0				-0.274632
				-1.0			-0.343395
				-1.5			-0.267990
				-2.0			-0.220133
					0.02		-0.537290
					0.03		-0.594186
					0.04		-0.653895
						0.02	-0.509306
						0.03	-0.536726
						0.04	-0.565388

**Table 6**  
 Local Nusselt number for various embedding parameter values

$Ec$	$We$	$\alpha$	$M$	$\delta_1$	$\delta_2$	$\delta_3$	$\phi_1$	$\phi_2$	$Nu/Re$
0.2	0.2	0.2	0.1	0.5	-0.5	0.1	0.01	0.01	0.688776
				1.0					0.635446
				1.5					0.589220
				2.0					0.550761
					-1.0				0.607198
					-1.5				0.546547
					-2.0				0.506790
						0.5			0.534817
						1.0			0.418020
						1.5			0.343094
							0.02		0.718239
							0.03		0.747014
							0.04		0.775416
								0.02	0.693491
								0.03	0.698105
								0.04	0.702640

## 5. Conclusions

This study analyzed the impact of Wu's slip and Smoluchowski's temperature jump slip on the hybridization tangent hyperbolic nanofluid  $TiO_2/Ag$ . A mathematical formulation of the fluid flow over a stretching plate is developed to model the heat transfer fluid (HTF) in a solar collector. The governing partial differential equations have been transformed into nonlinear ordinary differential equations, and we have applied the HAM method to calculate the semi-analytical solutions to the problem. The influence of the embedded essential parameters, such as the first and second-order slip number and Smoluchowski's parameters on the temperature and velocity profile has been explicitly demonstrated and deliberated. Based on the results of this investigation, we can conclude:

- i.  $\delta_1$  and  $\delta_2$ , have a negative function with the velocity profile.  $\delta_1$  reduces the velocity profile by about 43.33%, while 51.61% of the velocity profile is decreased by  $\delta_2$
- ii.  $\delta_1$  and  $\delta_2$ , give a positive function with the temperature distribution
- iii.  $\delta_3$  reduces 42% of the temperature profile
- iv. The local skin friction is enhanced by  $\delta_2$  and  $\delta_1$ .
- v. The nanoparticles  $\phi_1$  and  $\phi_2$  volume fraction, respectively, decline the local skin friction but increase the heat transfer rate.
- vi.  $\delta_1$ ,  $\delta_2$  and  $\delta_3$  diminishes the local Nusselt number.

Overall, these parameters have a significant impact on the behavior of the HTF in the solar collector. The finding in the present study provides valuable insights into the fundamental understanding of fluid dynamics and heat transfer in hybrid nanofluids, which can be used to enhance the efficiency and performance of solar collectors.

## Acknowledgment

The current research has received financial support through vote numbers UTM Encouragement Research (UTMER) (Q.J130000.3854.31J28). I am deeply grateful to the Research Management Centre-UTM at Universiti Teknologi Malaysia (UTM) for their kind approval of the research grant,

which has provided crucial support for the project. I would also like to extend my appreciation to the members of the Fluid Mechanics Research Group UTM for their valuable advice and unwavering support.

## References

- [1] Choi, S. U.S., and Jeffrey A. Eastman. *Enhancing thermal conductivity of fluids with nanoparticles*. No. ANL/MSD/CP-84938; CONF-951135-29. Argonne National Lab.(ANL), Argonne, IL (United States), 1995.
- [2] Choi, S. U. S., Z. George Zhang, WLockwoodFE Yu, F. E. Lockwood, and E. A. Grulke. "Anomalous thermal conductivity enhancement in nanotube suspensions." *Applied physics letters* 79, no. 14 (2001): 2252-2254. <https://doi.org/10.1063/1.1408272>
- [3] Ali, Hafiz Muhammad, ed. *Hybrid nanofluids for convection heat transfer*. Academic Press, 2020.
- [4] Maskeen, Muhammad Muddassar, Ahmad Zeeshan, Obaid Ullah Mehmood, and Mohsan Hassan. "Heat transfer enhancement in hydromagnetic alumina–copper/water hybrid nanofluid flow over a stretching cylinder." *Journal of Thermal Analysis and Calorimetry* 138 (2019): 1127-1136. <https://doi.org/10.1007/s10973-019-08304-7>
- [5] Yıldız, Çağatay, Müslüm Arıcı, and Hasan Karabay. "Comparison of a theoretical and experimental thermal conductivity model on the heat transfer performance of Al<sub>2</sub>O<sub>3</sub>-SiO<sub>2</sub>/water hybrid-nanofluid." *International Journal of Heat and Mass Transfer* 140 (2019): 598-605. <https://doi.org/10.1016/j.ijheatmasstransfer.2019.06.028>
- [6] Waini, Iskandar, Anuar Ishak, and Ioan Pop. "MHD flow and heat transfer of a hybrid nanofluid past a permeable stretching/shrinking wedge." *Applied Mathematics and Mechanics* 41, no. 3 (2020): 507-520. <https://doi.org/10.1007/s10483-020-2584-7>
- [7] Minea, A. A., and M. G. Moldoveanu. "Overview of hybrid nanofluids development and benefits." *Journal of Engineering Thermophysics* 27 (2018): 507-514. <https://doi.org/10.1134/S1810232818040124>
- [8] Minea, Alina Adriana, and Wael M. El-Maghlany. "Influence of hybrid nanofluids on the performance of parabolic trough collectors in solar thermal systems: recent findings and numerical comparison." *Renewable Energy* 120 (2018): 350-364. <https://doi.org/10.1016/j.renene.2017.12.093>
- [9] Hu, Guangtao, Xing Ning, Muzamil Hussain, Uzair Sajjad, Muhammad Sultan, Hafiz Muhammad Ali, Tayyab Raza Shah, and Hassaan Ahmad. "Potential evaluation of hybrid nanofluids for solar thermal energy harvesting: A review of recent advances." *Sustainable Energy Technologies and Assessments* 48 (2021): 101651. <https://doi.org/10.1016/j.seta.2021.101651>
- [10] Ahmadi, Mohammad Hossein, Mahyar Ghazvini, Milad Sadeghzadeh, Mohammad Alhuyi Nazari, and Mohammad Ghalandari. "Utilization of hybrid nanofluids in solar energy applications: a review." *Nano-Structures & Nano-Objects* 20 (2019): 100386. <https://doi.org/10.1016/j.nanoso.2019.100386>
- [11] Shah, Tayyab Raza, and Hafiz Muhammad Ali. "Applications of hybrid nanofluids in solar energy, practical limitations and challenges: a critical review." *Solar energy* 183 (2019): 173-203. <https://doi.org/10.1016/j.solener.2019.03.012>
- [12] Xiong, Qingang, Sam Altnji, Tahar Tayebi, Mohsen Izadi, Ahmad Hajjar, Bengt Sundén, and Larry KB Li. "A comprehensive review on the application of hybrid nanofluids in solar energy collectors." *Sustainable Energy Technologies and Assessments* 47 (2021): 101341. <https://doi.org/10.1016/j.seta.2021.101341>
- [13] Xuan, Yimin, Huiling Duan, and Qiang Li. "Enhancement of solar energy absorption using a plasmonic nanofluid based on TiO<sub>2</sub>/Ag composite nanoparticles." *Rsc Advances* 4, no. 31 (2014): 16206-16213. <https://doi.org/10.1039/C4RA00630E>
- [14] Li, Wenjing, Yixin Wang, and Changjun Zou. "Stability, thermal conductivity and supercooling behavior of novel  $\beta$ -CD-TiO<sub>2</sub>-Ag cooling medium-based nanofluids for eco-friendly cold thermal energy storage." *Journal of Cleaner Production* 259 (2020): 121162. <https://doi.org/10.1016/j.jclepro.2020.121162>
- [15] Bakar, Shahirah Abu, Norihan Md Arifin, Norfifah Bachok, and Fadzilah Md Ali. "Effect of thermal radiation and MHD on hybrid Ag–TiO<sub>2</sub>/H<sub>2</sub>O nanofluid past a permeable porous medium with heat generation." *Case Studies in Thermal Engineering* 28 (2021): 101681. <https://doi.org/10.1016/j.csite.2021.101681>
- [16] Rashid, Umair, Haiyi Liang, Hijaz Ahmad, Muhammad Abbas, Azhar Iqbal, and Yasser Salah Hamed. "Study of (Ag and TiO<sub>2</sub>)/water nanoparticles shape effect on heat transfer and hybrid nanofluid flow toward stretching shrinking horizontal cylinder." *Results in Physics* 21 (2021): 103812. <https://doi.org/10.1016/j.rinp.2020.103812>
- [17] Jamshed, Wasim, M. Prakash, S. Suriya Uma Devi, Rabha W. Ibrahim, Faisal Shahzad, Kottakkaran Sooppy Nisar, Mohamed R. Eid, Abdel-Haleem Abdel-Aty, M. Motawi Khashan, and I. S. Yahia. "A brief comparative examination of tangent hyperbolic hybrid nanofluid through a extending surface: numerical Keller–Box scheme." *Scientific Reports* 11, no. 1 (2021): 24032. <https://doi.org/10.1038/s41598-021-03392-8>
- [18] Kho, Yap Bing, Rahimah Jusoh, Mohd Zuki Salleh, Muhammad Khairul Anuar Mohamed, Zulkhibri Ismail, and Rohana Abdul Hamid. "Inclusion of viscous dissipation on the boundary layer flow of Cu-TiO<sub>2</sub> hybrid nanofluid over

- stretching/shrinking sheet." *Journal of Advanced Research in Fluid Mechanics and Thermal Sciences* 88, no. 2 (2021): 64-79. <https://doi.org/10.37934/arfmts.88.2.6479>
- [19] Teh, Yuan Ying, and Adnan Ashgar. "Three dimensional MHD hybrid nanofluid Flow with rotating stretching/shrinking sheet and Joule heating." *CFD Letters* 13, no. 8 (2021): 1-19. <https://doi.org/10.37934/cfdl.13.8.119>
- [20] Reddy, N. Keerthi, HA Kumara Swamy, M. Sankar, and Bongsoo Jang. "MHD convective flow of Ag–TiO<sub>2</sub> hybrid nanofluid in an inclined porous annulus with internal heat generation." *Case Studies in Thermal Engineering* 42 (2023): 102719. <https://doi.org/10.1016/j.csite.2023.102719>
- [21] Kho, Yap Bing, Rahimah Jusoh, Mohd Zuki Salleh, Mohd Hisyam Ariff, and Nooraini Zainuddin. "Magnetohydrodynamics flow of Ag-TiO<sub>2</sub> hybrid nanofluid over a permeable wedge with thermal radiation and viscous dissipation." *Journal of Magnetism and Magnetic Materials* 565 (2023): 170284. <https://doi.org/10.1016/j.jmmm.2022.170284>
- [22] Ahmad, Salman. "Computational analysis of comparative heat transfer enhancement in Ag-H<sub>2</sub>O, TiO<sub>2</sub>-H<sub>2</sub>O and Ag-TiO<sub>2</sub>-H<sub>2</sub>O: Finite difference scheme." *Journal of the Taiwan Institute of Chemical Engineers* 142 (2023): 104672.
- [23] Wu, Lin. "A slip model for rarefied gas flows at arbitrary Knudsen number." *Applied Physics Letters* 93, no. 25 (2008). <https://doi.org/10.1063/1.3052923>
- [24] Fang, Tiegang, and Abdul Aziz. "Viscous flow with second-order slip velocity over a stretching sheet." *Zeitschrift für Naturforschung A* 65, no. 12 (2010): 1087-1092. <https://doi.org/10.1515/zna-2010-1212>
- [25] Fang, Tiegang, Shanshan Yao, Ji Zhang, and Abdul Aziz. "Viscous flow over a shrinking sheet with a second order slip flow model." *Communications in Nonlinear Science and Numerical Simulation* 15, no. 7 (2010): 1831-1842. <https://doi.org/10.1016/j.cnsns.2009.07.017>
- [26] Khan, Sami Ullah, H. Waqas, S. A. Shehzad, and M. Imran. "Theoretical analysis of tangent hyperbolic nanoparticles with combined electrical MHD, activation energy and Wu's slip features: a mathematical model." *Physica Scripta* 94, no. 12 (2019): 125211. <https://doi.org/10.1088/1402-4896/ab399f>
- [27] Shaw, S., Ali J. Chamkha, A. Wakif, O. D. Makinde, and M. K. Nayak. "Effects of Wu's slip and non-uniform source/sink on entropy optimized radiative Magnetohydrodynamic up/down flow of Nanofluids." *Journal of Nanofluids* 11, no. 3 (2022): 305-317. <https://doi.org/10.1166/jon.2022.1840>
- [28] Farooq, Umar, Hassan Waqas, Roa Makki, Mohamed R. Ali, Abdullah Alhushaybari, Taseer Muhammad, and Muhammad Imran. "Computation of Cattaneo-Christov heat and mass flux model in Williamson nanofluid flow with bioconvection and thermal radiation through a vertical slender cylinder." *Case Studies in Thermal Engineering* 42 (2023): 102736. <https://doi.org/10.1016/j.csite.2023.102736>
- [29] Nandeppanavar, Mahantesh M., K. Vajravelu, M. Subhas Abel, and M. N. Siddalingappa. "Second order slip flow and heat transfer over a stretching sheet with non-linear Navier boundary condition." *International Journal of Thermal Sciences* 58 (2012): 143-150. <https://doi.org/10.1016/j.ijthermalsci.2012.02.019>
- [30] Khan, Sami Ullah, H. Waqas, M. M. Bhatti, and M. Imran. "Bioconvection in the rheology of magnetized couple stress nanofluid featuring activation energy and Wu's slip." *Journal of Non-Equilibrium Thermodynamics* 45, no. 1 (2020): 81-95. <https://doi.org/10.1515/jnet-2019-0049>
- [31] Mabood, Fazle, and Antonio Mastroberardino. "Melting heat transfer on MHD convective flow of a nanofluid over a stretching sheet with viscous dissipation and second order slip." *Journal of the Taiwan Institute of Chemical Engineers* 57 (2015): 62-68. <https://doi.org/10.1016/j.jtice.2015.05.020>
- [32] Roşca, Alin V., and Ioan Pop. "Flow and heat transfer over a vertical permeable stretching/shrinking sheet with a second order slip." *International Journal of Heat and Mass Transfer* 60 (2013): 355-364. <https://doi.org/10.1016/j.ijheatmasstransfer.2012.12.028>
- [33] Rahman, M. M., A. V. Roşca, and I. Pop. "Boundary layer flow of a nanofluid past a permeable exponentially shrinking/stretching surface with second order slip using Buongiorno's model." *International Journal of Heat and Mass Transfer* 77 (2014): 1133-1143. <https://doi.org/10.1016/j.ijheatmasstransfer.2014.06.013>
- [34] Uddin, Mohammed Jashim, Yasser Alginahi, O. Anwar Bég, and Muhammad Nomani Kabir. "Numerical solutions for gyrotactic bioconvection in nanofluid-saturated porous media with Stefan blowing and multiple slip effects." *Computers & Mathematics with Applications* 72, no. 10 (2016): 2562-2581. <https://doi.org/10.1016/j.camwa.2016.09.018>
- [35] Li, Yun-Xiang, Hassan Waqas, Kamel Al-Khaled, Shan Ali Khan, M. Ijaz Khan, Sami Ullah Khan, Rabia Naseem, and Yu-Ming Chu. "Simultaneous features of Wu's slip, nonlinear thermal radiation and activation energy in unsteady bio-convective flow of Maxwell nanofluid configured by a stretching cylinder." *Chinese Journal of Physics* 73 (2021): 462-478. <https://doi.org/10.1016/j.cjph.2021.07.033>
- [36] Le, Nam TP, Ngoc Anh Vu, and Le Tan Loc. "New type of Smoluchowski temperature jump condition considering the viscous heat generation." *AIAA Journal* 55, no. 2 (2017): 474-483. <https://doi.org/10.2514/1.J055058>

- [37] Assam, Ashwani, Nikhil Kalkote, Nishanth Dongari, and Vinayak Eswaran. "Comprehensive evaluation of a new type of smoluchowski temperature jump condition." *AIAA Journal* 56, no. 11 (2018): 4621-4625. <https://doi.org/10.2514/1.J057385>
- [38] Sajid, Tanveer, M. Sagheer, and Shafqat Hussain. "Role of Maxwell velocity and smoluchowski temperature jump slip boundary conditions to non-Newtonian Carreau fluid." *Frontiers in Heat and Mass Transfer (FHMT)* 14 (2020). <https://doi.org/10.5098/hmt.14.28>
- [39] Sajid, Tanveer, Wasim Jamshed, Faisal Shahzad, Esra Karatas Akgül, Kottakkaran Sooppy Nisar, and Mohamed R. Eid. "Impact of gold nanoparticles along with Maxwell velocity and Smoluchowski temperature slip boundary conditions on fluid flow: Sutterby model." *Chinese Journal of Physics* 77 (2022): 1387-1404. <https://doi.org/10.1016/j.cjph.2021.11.011>
- [40] Atif, S. M., Homan Emadifar, H. Günerhan, and F. H. Oyelami. "Effect of Maxwell Velocity and Smoluchowski Temperature Jump Slip Conditions on Tangent Hyperbolic Nanofluid." *Mathematical Problems in Engineering* 2022 (2022). <https://doi.org/10.1155/2022/2158509>
- [41] Hussain, Syed M., Wasim Jamshed, and Mohamed R. Eid. "Solar-HVAC thermal investigation utilizing (Cu-AA7075/C6H9NaO7) MHD-driven hybrid nanofluid rotating flow via second-order convergent technique: A novel engineering study." *Arabian Journal for Science and Engineering* 48, no. 3 (2023): 3301-3322. <https://doi.org/10.1007/s13369-022-07140-6>
- [42] Jamshed, Wasim, Mohamed R. Eid, Rabia Safdar, Amjad Ali Pasha, Siti Suzilliana Putri Mohamed Isa, Mohammad Adil, Zulfiqar Rehman, and Wajaree Weera. "RETRACTED ARTICLE: Solar energy optimization in solar-HVAC using Sutterby hybrid nanofluid with Smoluchowski temperature conditions: a solar thermal application." *Scientific Reports* 12, no. 1 (2022): 11484. <https://doi.org/10.1038/s41598-022-15685-7>
- [43] Wahid, Nur Syahirah, Nor Aliza Abd Rahmin, Norihan Md Arifin, Najiyah Safwa Khashi'ie, Ioan Pop, Norfifah Bachok, and Mohd Ezad Hafidz Hafidzuddin. "Radiative Blasius Hybrid Nanofluid Flow Over a Permeable Moving Surface with Convective Boundary Condition." *Journal of Advanced Research in Fluid Mechanics and Thermal Sciences* 100, no. 3 (2022): 115-132. <https://doi.org/10.37934/arfmts.100.3.115132>
- [44] Xue, Q. Z. "Model for thermal conductivity of carbon nanotube-based composites." *Physica B: Condensed Matter* 368, no. 1-4 (2005): 302-307. <https://doi.org/10.1016/j.physb.2005.07.024>
- [45] Ishtiaq, Bushra, Ahmed M. Zidan, Sohail Nadeem, and Mohammed Kbiri Alaoui. "Scrutinization of MHD stagnation point flow in hybrid nanofluid based on the extended version of Yamada-Ota and Xue models." *Ain Shams Engineering Journal* 14, no. 3 (2023): 101905. <https://doi.org/10.1016/j.asej.2022.101905>
- [46] Liao, Shi-Jun. "An approximate solution technique not depending on small parameters: a special example." *International Journal of Non-Linear Mechanics* 30, no. 3 (1995): 371-380. [https://doi.org/10.1016/0020-7462\(94\)00054-E](https://doi.org/10.1016/0020-7462(94)00054-E)
- [47] Liao, Shi-Jun. "An explicit, totally analytic approximate solution for Blasius' viscous flow problems." *International Journal of Non-Linear Mechanics* 34, no. 4 (1999): 759-778. [https://doi.org/10.1016/S0020-7462\(98\)00056-0](https://doi.org/10.1016/S0020-7462(98)00056-0)
- [48] Dawar, Abdullah, Saeed Islam, Ahmed Alshehri, Ebenezer Bonyah, and Zahir Shah. "Heat transfer analysis of the MHD stagnation point flow of a non-Newtonian tangent hyperbolic hybrid nanofluid past a non-isothermal flat plate with thermal radiation effect." *Journal of Nanomaterials* 2022 (2022): 1-12. <https://doi.org/10.1155/2022/4903486>
- [49] Ganesh Kumar, K., B. J. Giresha, and R. S. R. Gorla. "Flow and heat transfer of dusty hyperbolic tangent fluid over a stretching sheet in the presence of thermal radiation and magnetic field." *International Journal of Mechanical and Materials Engineering* 13, no. 1 (2018): 1-11. <https://doi.org/10.1186/s40712-018-0088-8>
- [50] Akbar, Noreen Sher, S. Nadeem, R. Ul Haq, and Z. H. Khan. "Numerical solutions of magnetohydrodynamic boundary layer flow of tangent hyperbolic fluid towards a stretching sheet." *Indian journal of Physics* 87 (2013): 1121-1124. <https://doi.org/10.1007/s12648-013-0339-8>
- [51] Ibrahim, Wubshet. "Magnetohydrodynamics (MHD) flow of a tangent hyperbolic fluid with nanoparticles past a stretching sheet with second order slip and convective boundary condition." *Results in physics* 7 (2017): 3723-3731. <https://doi.org/10.1016/j.rinp.2017.09.041>
- [52] Fathizadeh, M., M. Madani, Yasir Khan, Naeem Faraz, Ahmet Yildirim, and Serap Tutkun. "An effective modification of the homotopy perturbation method for MHD viscous flow over a stretching sheet." *Journal of King Saud University-Science* 25, no. 2 (2013): 107-113. <https://doi.org/10.1016/j.jksus.2011.08.003>
- [53] Ali, Mohamed E. "The effect of variable viscosity on mixed convection heat transfer along a vertical moving surface." *International Journal of Thermal Sciences* 45, no. 1 (2006): 60-69. <https://doi.org/10.1016/j.ijthermalsci.2005.04.006>
- [54] Chen, C-H. "Laminar mixed convection adjacent to vertical, continuously stretching sheets." *Heat and Mass transfer* 33 (1998): 471-476. <https://doi.org/10.1007/s002310050217>



- [55] Patil, P. M., and Madhavarao Kulkarni. "Analysis of MHD mixed convection in a Ag-TiO<sub>2</sub> hybrid nanofluid flow past a slender cylinder." *Chinese Journal of Physics* 73 (2021): 406-419. <https://doi.org/10.1016/j.cjph.2021.07.030>